

Article

Transfemoral Amputee Stumble Detection through Machine-Learning Classification: Initial Exploration with Three Subjects

Lucas Galey ^{1,*} , Olac Fuentes ² and Roger V. Gonzalez ¹

¹ Engineering Education and Leadership, The University of Texas at El Paso, El Paso, TX 79968, USA; rvgonzalez@utep.edu

² Computer Science, The University of Texas at El Paso, El Paso, TX 79968, USA

* Correspondence: ljgaley@miners.utep.edu or lucasgaley@hotmail.com

Abstract: Objective: To train a machine-learning (ML) algorithm to classify stumbling in transfemoral amputee gait. Methods: Three subjects completed gait trials in which they were induced to stumble via three different means. Several iterations of ML algorithms were developed to ultimately classify whether individual steps were stumbles or normal gait using leave-one-out methodology. Data cleaning and hyperparameter tuning were applied. Results: One hundred thirty individual stumbles were marked and collected during the trials. Single-layer networks including Long-Short Term Memory (LSTM), Simple Recurrent Neural Network (SimpleRNN), and Gradient Recurrent Unit (GRU) were evaluated at 76% accuracy (LSTM and GRU). A four-layer LSTM achieved an 88.7% classic accuracy, with 66.9% step-specific accuracy. Conclusion: This initial trial demonstrated the ML capabilities of the gathered dataset. Though further data collection and exploration would likely improve results, the initial findings demonstrate that three forms of induced stumble can be learned with some accuracy. Significance: Other datasets and studies, such as that of Chereshev et al. with HuGaDB, demonstrate the cataloging of human gait activities and classifying them for activity prediction. This study suggests that the integration of stumble data with such datasets would allow a knee prosthesis to detect stumbles and adapt to gait activities with some accuracy without depending on state-based recognition.



Citation: Galey, L.; Fuentes, O.; Gonzalez, R.V. Transfemoral Amputee Stumble Detection through Machine-Learning Classification: Initial Exploration with Three Subjects.

Prosthesis **2024**, *6*, 235–250. <https://doi.org/10.3390/prosthesis6020018>

Academic Editors: Marco Cicciu and Giuseppina Gini

Received: 14 December 2023

Revised: 20 February 2024

Accepted: 27 February 2024

Published: 4 March 2024



Copyright: © 2024 by the authors. Licensee MDPI, Basel, Switzerland. This article is an open access article distributed under the terms and conditions of the Creative Commons Attribution (CC BY) license (<https://creativecommons.org/licenses/by/4.0/>).

Keywords: artificial knee; machine learning; prosthesis; stumble recognition; recovery

1. Introduction

Current advanced prosthetic knee technology uses kinematic detection with discrete state-based control to modulate gait activities [1,2]. However, unforeseen surfaces or obstacles are by nature chaotic and do not always exhibit a recognized kinematic warning. Consequently, amputees stumble and often fall, since the knee system does not react and offer support. Fear of falling affects approximately half of lower-limb amputees [3]. Statistically, even though active knees show an improvement over passive knees in falling, almost all patients still fall [4,5], and more than 50% of lower-limb patients report falling at least once a year [6]. Therefore, systems that can accurately detect stumbles are needed to inform knee control to prevent falls. Though future work may include external sensing for truly predictive results, this research focuses on a novel interpretation of prosthetic knee industry standard kinematic data.

Key defining gait characteristics have been well documented by the literature both in individuals with a healthy gait and those with pathological diagnoses, such as cerebral palsy or muscular dystrophy [7–11]. Due to these distinctions, gait classification has grown in applied machine learning (ML), specifically in the differentiation between healthy and pathological gait [12–14]. Likewise, gait activity, such as walking, running, and standing, has been documented by datasets such as HuGaDB and classified by ML algorithms with high success levels (Badawi et al.: accuracy: 98.6%; Keçeci et al.: accuracy: >99% with many networks) [15–17].

Stumbles have been studied for many years with various levels of intensity. To date, there are eight stumble studies involving able-bodied subjects [18–25]. Though some numbers were difficult to ascertain from methods, the number of subjects in these studies ranged from 4 to 18 (avg: 8 ± 4), and each subject stumbled between 1 and 27 times (avg: 11 ± 9). The most common methods of stumble induction were an obstacle, a line, or a treadmill perturbation. For the most part, these were set at either a preprogrammed position or gait phase.

Among transfemoral amputees, there are more variables to consider, like knee type and stumble side (intact or prosthetic). Fewer stumble studies were found for transfemoral amputees, and the methodology was often not clearly delineated. Though there are some assumptions with the able-bodied subject trials, several of the amputee subject trials have stumbling time or summative stumbles. The studies had on average nine subjects (± 6) but were often mixed between transfemoral and able-bodied subjects [26–33]. Outside of two studies, the average amount of stumbles was six (± 4), and repeatability is further reduced by the stumbles being split across leg sides and types of knees. Those two studies, though both still with mixed subject pools (including transtibial), included a large quantity of induced stumbles [32,34], with the study by Shirota et al. having high levels of repeatability of 36 stumbles per amputee per side with only one knee tested. The study by Shawen et al. was much less repeatable, with stumble induction methods ranging from self-induced tripping to poorly defined pushes from the side, but still inducing stumbles 36 times per amputee. These two studies offer a large pool of stumble inductions but are both limited in variance of the controlled induction type and in scope of the knee systems compared repeatably.

Additionally, the literature shows several implementations of real-time gait event detections using sensors and many more gait activity classifications with potential for real-time applications [35–39]. However, with the limitation of studies that measure stumble characteristics, especially constrained to patients with amputations, no studies have been found that attempt to classify stumbles in gait in real time. Even most gait activity studies are limited to postliminary processing. The work presented in this study seeks to fill that gap, both by beginning to provide the gait data pertaining to transfemoral amputees during stumble events and by presenting a first approach to classifying stumble and gait events using ML. The scope of the research is constrained to signals and parameters that can be measured and implemented into electromechanical prosthetic knee systems, such as the one developed by some of the authors [40]. The goal is that early, real-time recognition of stumbles will lead to fall prevention by influencing prosthetic knee control systems.

1.1. Gait Data

Some of the most complete research conducted in gait analysis was by Sagawa et al., who reviewed the preferred biomechanical and physiological parameters that are most often used in determining gait characteristics. Though their results were inconclusive, the most common parameters pertaining to the knee joint were oxygen consumption, knee flexion angle, gait velocity, cadence, stride length, stance time, and maximum vertical ground reaction force [41]. Though some of these parameters are not feasible to measure within a prosthetic knee system, the following sensors are commonly used to determine knee joint parameters: accelerometers [21,42,43], gyroscopes [42,44], goniometers [45,46], magnetometers [47], and linear sensors (i.e., hall pass or linear potentiometer). Therefore, this research centered on using an IMU that contains three axes as the foundational component to capture kinematic data: an accelerometer, a gyroscope, and a magnetometer.

1.2. Machine-Learning Networks

As stated previously, ML networks have been successful in classifying a variety of gait types and conditions and differentiating between gait activities. The types of networks used have varied between nearest neighbor, random forest, neural networks, and combinations of those and more. Fundamentally, the classifications of those networks have focused on

gait mode classification (walking, running, etc.). Though the input data are time-dependent, gait mode classification is not considered a forecasting task in itself.

However, real-time prediction, as presented in the current research, does involve forecasting and gait classification due to the machine's requirement to use a continuous time-dependent data stream to predict gait mode. To do this, forecasting on a time series requires different configurations or types of ML networks that retain information from previous predictions known as recurrent neural networks (RNN). A popular RNN is Long Short-Term Memory (LSTM) [48].

LSTMs, shown in Figure 1, function by using three types of data gates within each memory block: forget, remember/input, and output. As time progresses, the network retains previous information via two recurrent states, the memory state and the hidden state. The blocks of the network receive the network input, the hidden output of the previous block, and the memory data stream from the previous block. Learning layers (memory blocks between the initial input and final output of the network) decide what information to forget from the data stream, what information to add to the data stream, and what prediction to make. The output is a combination of the current block's data stream and the block's prediction. The dependency on past predictions, coupled with the ability to discard old information, allows LSTMs to function in time series where the subsequent output depends on the previous output.

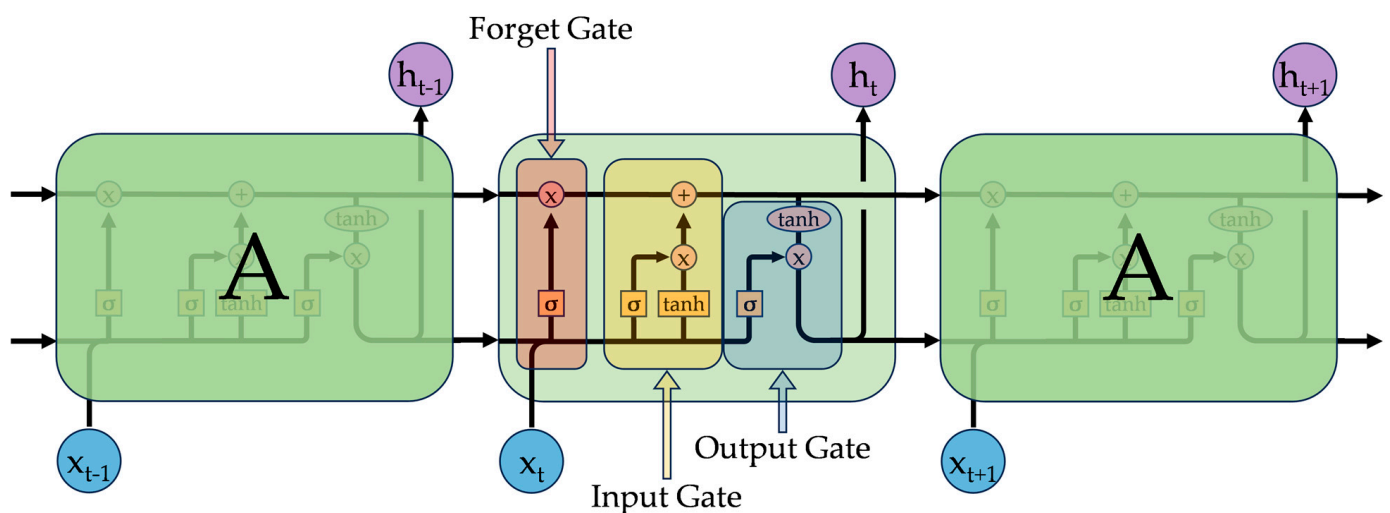


Figure 1. Visual representation of a Long Short-Term Memory (LSTM) network block. Image inspired by [49].

Though error functions are used to optimize a ML network, accuracy is often the metric used to evaluate the performance of the network. In addition to this, the F-score, precision, recall, and false positive rate (FPR) were also considered.

2. Methods

To train the ML network, data had to be collected, and classification labels added manually. Amputee gait and stumble data were collected using a sensor system embedded in a LIMBS M3 prosthetic knee. The sensor array was made of two nine degrees-of-freedom (DoF) sensors—one attached to the thigh and one to the shank segment of the knee (pictured in Figure 2). Each sensor recorded data from a unique perspective. From a position time perspective, the data progressed from position (magnetometer) to change in position (gyroscope) to the rate of velocity change (accelerometer).

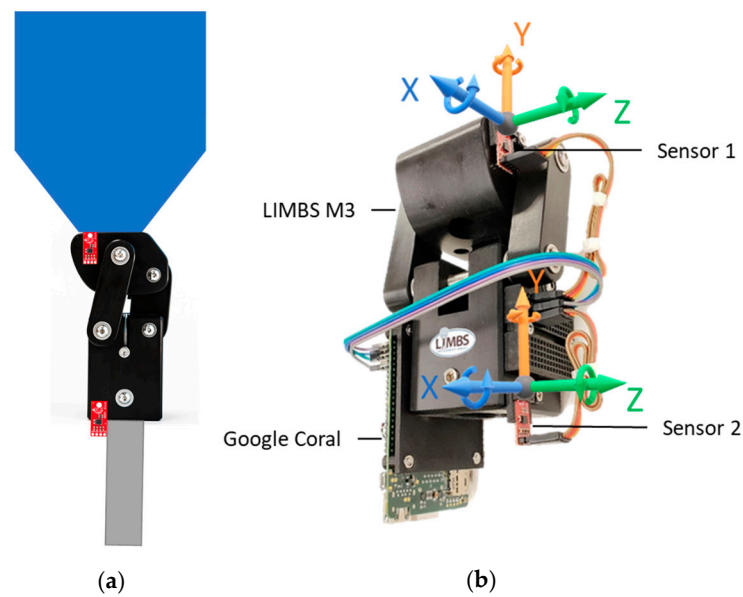


Figure 2. Data collection system. (a) Model with socket, sensor knee, and pylon. (b) Device with coordinate systems for the sensors.

Subjects were asked to walk at selected speeds on a treadmill while in a safety harness, and stumbles were induced in three different ways (shown in Figure 3): (1) to simulate inadequate leg momentum during a step, a bungee attached to the foot applied a breaking force to their prosthesis during gait; (2) to simulate tripping over an obstacle, a bumper was inserted in front of their prosthesis during gait; (3) to simulate uneven surfaces, an object was dropped onto the treadmill while the subject was stepping, which induced raised elevation, foot slipping, and small toe catches. Stumbles were induced during the second half of the prosthesis swing phase. These three events cover the primary forms of stumble during gait as described by the literature and aided in collecting a variety of stumble simulations to train the ML network to predict gait activity modes. For classification, the data were split into four events: walking, bungee stumble, obstacle stumble, and uneven stumble. Treadmill stumble induction is well established in the literature and is effective at inducing realistic stumbles [30].

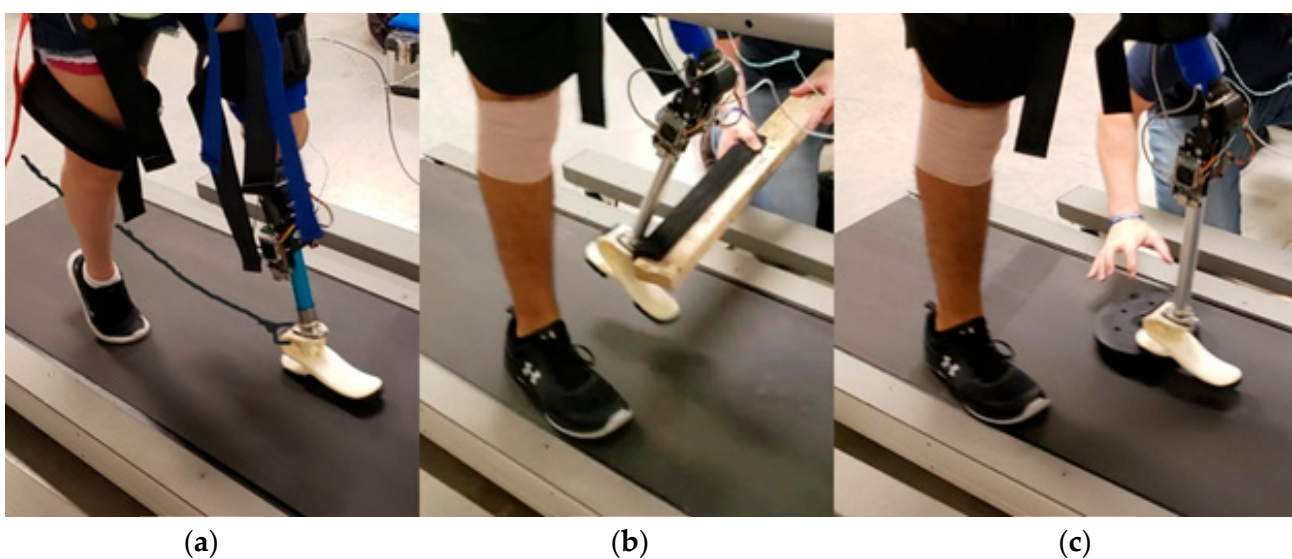


Figure 3. Examples of stumble induction for stumble with bungee: (a), obstacle (b) and stumble with uneven ground (c). Image (c) demonstrates stumble with a bungee and is a simulated image showing the attachment point.

2.1. Gait Trials

The study was reviewed and approved by The University of Texas at El Paso's (UTEPs) IRB for study 1329153-3. Four subjects consented to the study, but data were collected for three subjects before the study was permanently put on hold due to COVID-19. The three subjects are labeled S1, S2, and S4. Subject qualifying criteria were as follows: age between 21 and 60, unilateral transfemoral amputation, no secondary health conditions or neurological disorders, activity level of at least K3, and general good health.

The trials were conducted using the data collection system described below, along with a RTM600™ Rehabilitation Treadmill (Biodex, Shirley, NY, USA) and Unweighing Harness (Biodex, Shirley, NY, USA). The data collection system was made up of two nine-DoF Sensor Sticks (SparkFun Electronics, Niwot, CO, USA) and a Raspberry Pi 3 or Google Coral (Adafruit, New York City, NY, USA and Google, Mountain View, CA, USA). To prevent chances of injury, the harness was adjusted so that in the event of a fall, neither the patient's arms nor knees touched the ground.

The subjects were fit with a LIMBS M3 (LIMBS International, El Paso, TX, USA) knee that contained the sensor array and a Niagara Foot v1 (LIMBS International, El Paso, TX, USA) with a rubber sole. The array in no way impeded the normal movement of the prosthetic knee. A prosthetist fit the prosthetic appropriately during the trial.

Subjects were asked to walk at three self-selected speeds for five minutes and a final five minutes of walking at speeds that were varied within the self-selected speed ranges. This walk was without induced stumbles. After this acclimation period, the patients were asked to wear a pair of glasses that restricted their vision of the ground. These were worn to prevent the subjects from reflexively predicting stumbles as they saw them approaching. Patients were asked to walk normally at a speed they selected between 0.8 m/s and 1.5 m/s. Stumbles were induced during that time. The patients were asked to allow themselves to fall naturally until caught by the harness. This process continued until a minimum of 30 stumbles had been recorded. Finally, subjects were asked to stand for one minute while shifting their weight on and between legs.

Recorded Data

Each stumble event was recorded and tracked with the time of the data stream. The frequency of the data recording was 60 Hz. Data recordings from each sensor included three-dimensional sensor data of acceleration, velocity, and magnetic field for the prosthetic knee. The data collection system had one sensor attached to the thigh and one sensor attached to the shank. Each sensor was oriented for acceleration and magnetic field to be orthogonal to and velocity to be rotational on the frontal (X), transverse (Y), and sagittal (Z) planes with respect to the body segment. If the subjects stumbled, a researcher pressed a button that tracked stumble alongside the sensor data.

During data evaluation and preparation, it was observed that several of the tracked stumbles were not aligned with actual stumble induction. By observing all channels of sensor data, the stumbles were manually re-marked, and several were deleted for being indiscernible from normal gait. The distribution of the cleaned stumbles can be seen in the Results (Section 3).

The data for training recurrent networks were sampled into rows per each current timestep, which will be referred to as "samples". Each included both the current sensor data and 10 historic sensor data points equally distributed across the last 20 timesteps. During training, this row was reshaped into a matrix of features and timesteps for the input layer.

2.2. Machine Learning

The overarching method behind training the ML model was incremental testing with increasingly complex mechanisms. The ML architecture was implemented through Keras and TensorFlow [50,51]. Described below are the methods used, with specifics being found in the Methods (Section 2).

2.2.1. Classes

Fundamentally, the data had four classes: walking, stumbling by bungee, stumbling by obstacle, and stumbling by unevenness. However, the classes were also at times combined into simply walking and stumbling.

To train the networks, the data were split into training and testing datasets. Training sets were used to identify data stream patterns that lead to successful predictions; test sets were used to evaluate the model's performance. Because of the time series-dependent nature of the data and prediction sequences (motions leading up to a stumble or non-stumble are sequential and time-dependent), samples could not simply be randomized and split for training and testing. Rather, to avoid compromising network integrity, the train/test split used a leave-one-out (LOO) methodology. LOO views each subject as one complete case, and the process will iterate through all subjects as the test set. This eliminated the overlap of training and testing data and allowed the network to be trained on two subjects while predicting the events of the third iteratively. To offset data class imbalances, artificial data points were created during stumbling events based on raw data curve-fitting techniques.

Additionally, the classes of standing and sitting were deemed outside the scope of this project due to lack of data, proper evaluation methods, and impact on control methods. In the end, the remaining classes were a summative "stumble" and "walking".

2.2.2. Optimizing

A few methods were applied to increase accuracy and decrease the computational load. First, the features were evaluated, and it was determined that magnetometer data were not highly reproducible. Though easy to interpret and understand, magnetometer data are dependent on the sensor's orientation relative to the magnetic field of the earth. Therefore, the lab setup made the data for all three initial subjects comparable, but there was no guarantee that future tests would have similar and consistent orientations. Therefore, all six magnetometer features were eliminated after the initial model.

2.2.3. Hyperparameter Tuning

The final stage of network configuration was hyperparameter tuning within the bounds established by the earlier testing. The tuning was iterated through all the combinations of network parameters to optimize the network for this dataset. Table 1, below, highlights the parameters tuned, the ranges, and the steps. Training batch size was also evaluated separately within 60, 80, 120, 200, 400, and 600 samples. Hyperparameter evaluation was set to maximize accuracy and F-score. This was implemented through the KerasTuner [52].

Table 1. Hyperparameter tuning parameters.

Parameter	Min	Max	Step
LSTM 1 Units	25	500	25
LSTM 2 Units	25	500	25
Dense Units	25	500	25
Dropout Rate	0	0.9	0.1

All hyperparameters used to tune the model. Shown with minimum and maximum range and step size.

Various combinations of the different layers were also tried, with the layer orders being switched, disabled, or tuned individually. The hyperparameter output was evaluated for the top three combinations of values for each LOO dataset. The combination that was the most common across the different datasets was chosen as the final output.

2.2.4. Models

Classification of the data was performed in two major stages: initial and deployed. Neither of these stages represents one network, but rather they represent the result of many

iterations. A distinction is made between them, because the initial network was developed after an exploration of different ML algorithms and basic data-cleaning methods. The deployed network refined the basic methodology set by the initial network and implemented a more robust algorithm application.

Before the gait trials were conducted, the gait data from HuGaDB were explored and classified with a simple LSTM network. Because HuGaDB included similar data as intended to be used, namely, thigh and shank accelerometer and gyroscope data, the principles learned were applied to this study. Though the LSTM network was preselected for its success with the HuGaDB, Gradient Recurrent Unit (GRU) and Simple Recurrent Neural Network (SimpleRNN) were still tested in comparison by evaluating all three networks' performances with different networks sizes (50, 100, 200, and 400) and output layer activation functions (softmax, sigmoid, or none). This was done at the beginning with just an input and output layer model. For the recurrent networks, the data were transformed to include 10 past data points along with the current sensor sample.

Additionally, to model the rule-based method of commercial prosthetic knees, a "Simple Rule" classification model was developed. This model used a calculated knee angle (>25 deg) with knee angular velocity (>100 deg/s; extension) obtained from the sensors to determine step occurrences, particularly the leg extension phase. During each such extension, the model checked for three rules: bungee, obstacle, and uneven detection. Each used repeatable sensor information to establish whether that type of stumble occurred. When a stumble was detected, it would continue for 0.5 s after the last detection. This "Simple Rule" model was used as a baseline comparison for the ML developed through this study.

Thereafter, data were cleaned with a MinMax scaler that adjusted each data channel to fall between 0 and 1. It was fit to training data and applied to transform validation and test data. Training files were augmented with artificial data, and manually marked stumble data were used. Various learning rates and optimizers were attempted, but RMSprop, with its default learning rate of 0.0001, performed well most consistently.

The initial machine-learning algorithm applied to the collected data was a LSTM network with one input layer, four hidden layers, and one output layer. The layers were an 11 by 18 input array, 300-node LSTM hidden layer, a 200-node LSTM hidden layer, a 100-node dense hidden layer, a 0.9-dropout hidden layer, and a two-class output with softmax activation layer. The train length was 20 epochs with a categorical cross-entropy loss function using the RMSprop optimizer. Training involved the full 18 features from the sensors and included 10 historical data points. The three different forms of stumble were trained as one general "stumble" class. Because there were only three subjects, LOO was used; two subjects were used for training, and one for testing. For the purpose of training, the data collected during the induced stumbles were used. This data included both gait and stumble events at a roughly 9:1 ratio, though artificial data shifted that ratio to 4:1. The validation dataset was 15% of the training data. At this stage, one minute of non-stumble walking data from the test subject was added to the training data. This was thought to keep the algorithm from overfitting and to help the system be aware of the subject's specific gait.

After hyperparameter tuning, the deployed network retained all four hidden layers. The layer parameters chosen during tuning were an 11 by 12 input array, a 200-node LSTM hidden layer, a 50-node LSTM hidden layer, a 300-node dense hidden layer, a 0.1-dropout hidden layer, and a two-class output layer with softmax activation. The train length was 30 epochs with a categorical cross-entropy loss function using the RMSprop optimizer at a learning rate of 0.001. As before, the three different forms of stumbles were combined into one "stumble" class, and artificial stumble data were used to balance the data. Different from before, the cleaned stumble data were used, and the magnetometer data were excluded. As before, LOO was used in conjunction with a small batch of non-stumble walking data from the test subject. The sum of changes between the initial and deployed networks includes the following: hyperparameter tuning, feature reduction, manual data marking. Each LOO procedure was run three times, and the results were averaged.

2.2.5. Result Evaluation

Traditionally, ML algorithms are evaluated by various metrics, such as accuracy, precision, recall, and F-score, which all depend on the prediction to ground-truth comparison. The results given in the Data Classification of the results highlight this principle (Section 3.3). Yet, it became clear that for this application, the ground-truth comparisons were more difficult to ascertain. The marked stumbles were often not initiated at the most accurate time, nor did they end exactly when the stumbles were over. This phenomenon was one of the reasons why the stumble data used for training were cleaned manually. However, even with a cleaned stumble, the true positive prediction would often not coincide perfectly with a marker. This led to errors in accuracy. Since an improper reaction to a few false positive predictions could cause an artificial stumble, a different metric had to be applied. Therefore, instead of predictions evaluated against the ground truth on a rolling data sample basis, the predictions and ground truths were used to evaluate individual steps instead. Steps were identified using the cyclic angular velocity peaks from the data to identify the gait cycle. Within each step, the rolling samples were evaluated, and a small six-sample buffer was applied to eliminate spikes in FPs. If 80% of the six samples were positive, then the ML model was predicting a stumble for the step. This was essentially a first step toward the control system.

3. Results

The data shown in the subsequent subsections are the results of the three-patient trial discussed in the methods. Though data from subsequent studies would greatly enhance the results, those are outside of the objective of this research. The positive prediction class is “stumble”.

3.1. Data Collection

The data collection methodology described was successfully completed with three subjects. Subjects 1 and 4 were male, and subject 2 was female. All amputations were the result of trauma, but with no secondary gait complications. Height ranged from approximately 1.63 to 1.85 m, and weight from approximately 54 to 95 kg. For each subject, approximately 900 total steps were collected. Measurements and data recording all happened on the side of the prosthetic knee. Average stride length and frequency were 1.09 m (± 0.25) and 0.71 Hz (± 0.11). As mentioned in the methods, the stumbles were manually validated and re-marked, and some were eliminated. The table of stumble distributions is shown below in Table 2.

Table 2. Distribution of stumble event occurrences.

	Bungee	Obstacle	Uneven	TOTAL
SUBJECT 1	11 (−2)	5 (−0)	12 (−2)	24
SUBJECT 2	12 (−1)	18 (−1)	29 (−1)	56
SUBJECT 4	19 (−3)	20 (−0)	24 (−10)	50
TOTAL	42 (−6)	43 (−1)	65 (−13)	130

Instances per subject manually re-marked. Some stumbles were removed when there was no observable effect. Removed occurrences are marked (−n). Total is summed after removing ignored cases.

An example of stumbling during uneven ground induction can be seen in Figure 4 below. It displays the full sensor array data, grouped by sensor type and body segment, and the tracked stumble (horizontal red line). Additionally, approximate gait events (heel strike, mid-stance, and toe-off) and beginning of stumble (vertical red line) were added. These additions were estimates but reflect historical measurements and specific sensor indications.

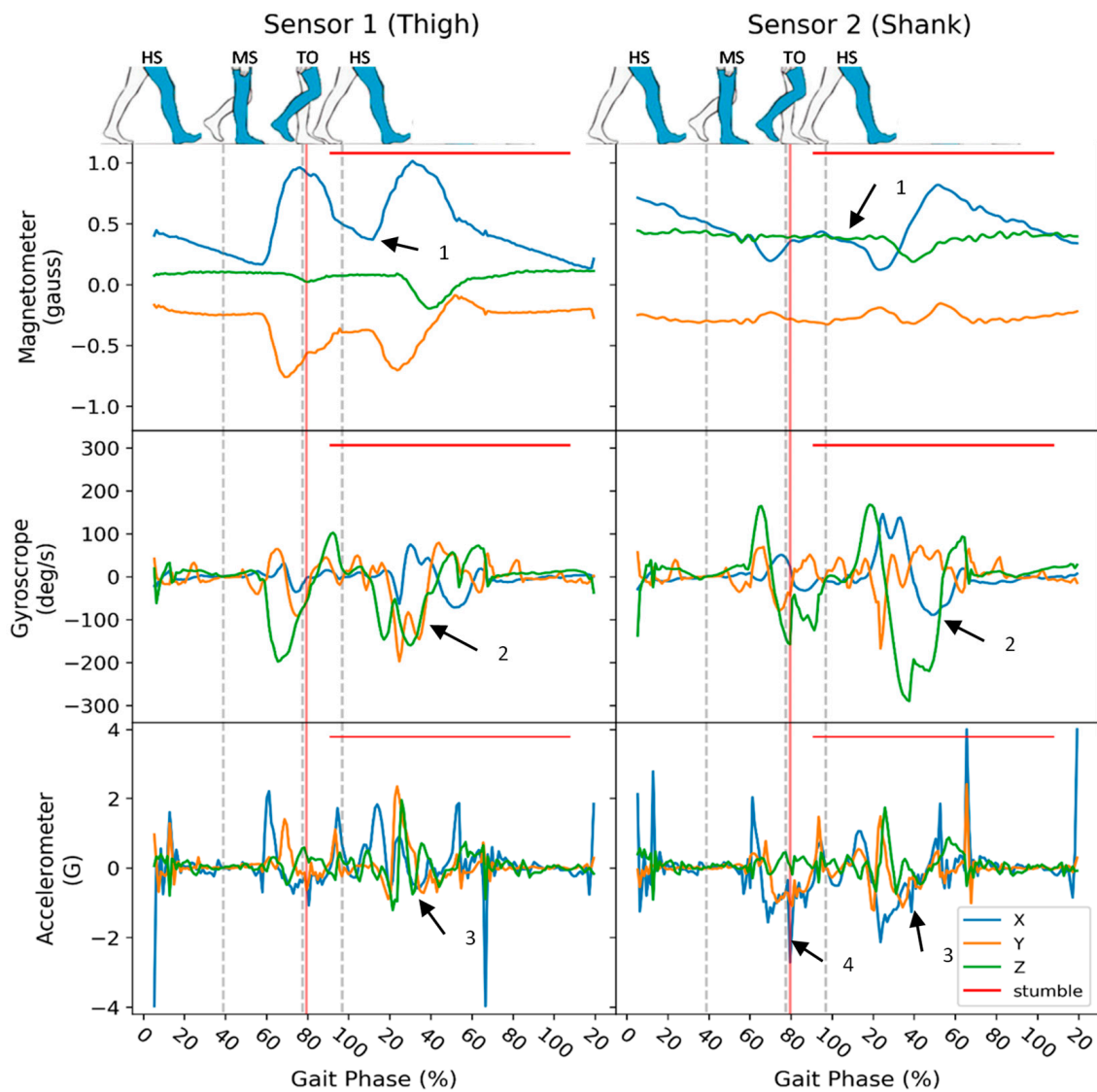


Figure 4. Sample of subject 1 prosthetic knee sensor data for stumble by uneven surface. Stumble data recording indicated by red horizontal line. Approximate beginning of actual stumble marked by vertical red line. Each column of graphs represents one sensor, and each row of graphs represents a sensor type. X, Y, and Z represent vectors orthogonal (accelerometer and magnetometer) and parallel (gyroscope) to the frontal (X), transverse (Y), and sagittal (Z) planes respective to the two body segments (thigh and shank). The horizontal axis shows the data respective to gait percentage and is cyclical. Vertical (gray) dotted lines represent key gait phase events of the prosthetic knee (blue). Gait events shown are heel strike (HS), mid-stance (MS), and toe-off (TO). Arrow 1 highlights magnetometer troughing, and arrow 2 highlights acceleration spikes from HS. Gait phase figures adapted from [53].

3.2. Machine-Learning Algorithm

This section describes the results of the initial data exploration methods implemented to improve the performance of the machine-learning model.

Data Exploration

The data below in Table 3 represent the first foray into different recurrent networks. SimpleRNN appears to not perform well despite the variances in structure. Though the results are very similar for GRU and LSTM, the previous experience with LSTM made it the more logical choice for continuation.

Table 3. Accuracy output of simple recurrent models.

Network	Net Size	Activation	Accuracy
LSTM	50	softmax	0.70
LSTM	100	softmax	0.71
LSTM	200	softmax	0.76
LSTM	50	sigmoid	0.70
LSTM	200	sigmoid	0.76
GRU	100	softmax	0.73
GRU	200	softmax	0.76
GRU	400	softmax	0.74
GRU	100	sigmoid	0.73
GRU	200	sigmoid	0.76
GRU	400	sigmoid	0.74
Simple Rule			0.79

Results for one recurrent layer (“Network”) and one dense layer for class output to walking and all three stumble modes. Data are filtered to show only accuracies above 0.70. The “Simple Rule” results for all three subjects are given in the last row.

Initially, three stumble classes were defined: obstacle, uneven, and bungee. However, preliminary work showed that specifying between these different types of stumbles decreased predictive power and increased error, and learning these classes ultimately led to overfitting. Therefore, all types of stumbling were combined into the one “stumble” class. Combining these classes led to an accuracy increase of 2% (78%) with a LSTM of size 200.

3.3. Data Classification

The classification results were split into two different models, “Initial” and “Deployed”. Both sets of results relate to the same dataset of three subjects. The improvements to these models have resulted in an increase in accuracy over the 78.8% of the “Simple Rule” baseline.

3.3.1. Initial

A network that was trained by subjects 1 and 2 and evaluated by subject 4 with no data overlap achieved an accuracy of 83.0%. In later trainings, the training data also included a one-minute sample of the variable speed walking, with no stumbles for the test subject (subject 4). The confusion matrix for this preliminary network is shown in Table 4. All metrics of the network increased, and there was an overall accuracy of 85.5%.

Table 4. Confusion matrix with walking data.

	Predicted		Recall	43.4%
ACTUAL	Bungee	Obstacle	Precision	69.9%
STUMBLE	1875	2444	FPR	4.5%
WALKING	809	17,275	F-score	53.5%
			ACCURACY	85.5%

Trained LSTM network including test subject walking data. Right column displays the evaluated metrics. Evaluated on subject 4.

3.3.2. Deployed

Table 5 shows the breakdown of the LOO training for each subject. It shows the network metrics, such as accuracy and recall, calculated in the typical sample-by-sample method. Additionally, it shows an analysis from the perspective of individual steps, with the metrics listed accordingly. Each subject’s data are the average of three trainings. Across all subjects, the classified stumbles lagged behind, marked by 0.09 (±0.11) s.

Table 5. LOO comparison and average.

Metric	Subject 1	Subject 2	Subject 4	Average
Network Accuracy	84.7%	87.8%	93.6%	88.7%
Network Precision	14.0%	32.2%	67.0%	37.7%
Network Recall	51.9%	50.5%	46.5%	49.6%
Network FPR	14.0%	9.1%	2.1%	8.4%
Network F1_Score	21.2%	37.9%	57.4%	38.8%
Total Steps	225	271	196	231
Total Stumbles	24	56	50	44
Caught Stumbles	23 (97%)	33 (57%)	41 (79%)	33 (73%)
False Stumbles	136 (60%)	54 (20%)	2 (1%)	64 (28%)
Step Accuracy	39.1%	70.7%	93.3%	66.9%
Step Precision	14.7%	38.0%	94.7%	33.8%
Step Recall	97.2%	57.5%	79.5%	73.1%
Step FPR	67.8%	25.6%	1.6%	31.7%
Step F1_Score	25.5%	45.8%	86.4%	46.2%

Deployed ML model. "Network" data are sample evaluation. Data include evaluation of step events. Each subject's data are an average of three runs of the same model.

4. Discussion

Though there is still a dearth of repeatable data, the literature suggests that amputees and able-bodied subjects react similarly to induced stumbles, typically by increasing gait frequency and decreasing step length following a perturbation [29,32]. Additionally, it appears that subjects with amputations still use the sensory information of the impact [32]. However, without the muscular control on the prosthetic leg, a new sudden step may not fully extend, which can lead to collapse. Therefore, the implementation of classification algorithms into intelligent prosthetic knees that seek emulate support-like intact leg responses should be established. To provide support and prevent falls, control systems should seek to accomplish the following: minimize knee angle at heel strike and provide stance support for quick recovery steps.

4.1. Gait Trials

It is important to note that though the beginning of the stumble was an estimate, so was the tracked stumble event. The tracked stumble events were recorded by a researcher when the stumbles were induced, and the subject stumbled. However, the bungee method had a significant delay between induction and actual stumble, whereas the obstacle was a near instantaneous stumble. Therefore, tracked events should be seen more as a highlighting of which gait cycle had stumbles as opposed to the exact instance of the stumble.

The various stumble modes were all selected to model scenarios encountered by amputees during normal gait. The bungee stumble was chosen to simulate a lack of adequate forward momentum of the prosthetic to lock the passive knee in preparation for heel strike. The data for this showed large spikes that are atypical for walking gait. The abnormal accelerations indicate rotation and imbalance.

The reactionary sensor data of stumbling with an obstacle do not seem to drastically vary from stumbling with a bungee. Gait imbalance is resolved very similarly to bungee stumble, and gait appears to resume. In both instances, it appears as though the subject did not fully extend the knee and quickly proceeded into a shaky flexion again.

Figure 4 shows stumbling with an uneven surface. This stumble has a diminished trough (arrow 1), yet it can be highlighted by arrow 2 that the subject has had a successful heel strike. This is supported by the spike in the X (orthogonal to transverse) acceleration and Z (sagittal plane) gyroscopes that can be seen in normal walking to accompany heel

strike. Although, as in the previous stumble modes, there were increases in acceleration and angular velocity indicating imbalance, the subject clearly recovered and completed a step. Though the subject had to accelerate their step frequency, the sensor data show that the subject resumed gait after stumbling.

4.2. Machine-Learning Classification

As seen in the results, the initial networks showed very little difference between GRU and LSTM. Even though the scores above 70% favored the GRU on average, the LSTM performed an equal maximum (76%) and was selected for its familiarity and success on predicting the HuGaDB dataset. The “Simple Rule” prediction performed better than all the initial ML models and was therefore used as a comparative standard. However, it was developed with very specific rules and likely would have been limited in its accuracy bounds. Once the ML models were diversified beyond input and output layers, the models quickly exceeded the 78.8% accuracy of the “Simple Rule” baseline model, with 83.0 and 85.5%. A rule-based model could likely be developed that approached such accuracies for stumbles, but the reliance on very specific conditions would plausibly limit its generalization. With a combination of the different stumble methods into one class, the ML models showed a generalization that would likely be applicable to chaotic stumbles that did not match defined expected stumble patterns.

Through the ML model development process, several oversights were discovered and addressed iteratively. This is to be expected when developing such a model. For instance, in typical machine learning, data are randomized and divided into training, testing, and validation sets. However, this dataset contains time series data with historic data points. Therefore, a randomized dataset could very well yield a train and test sample separated by milliseconds. This was addressed by LOO, but initially, many iterations of the network did not account for this. Previous experience with the similar HuGaDB dataset also encouraged the application of a similar successful ML network to this stumble dataset. Additionally, the original dataset was not cleaned to account for human error during the stumble marking. Though the methods of testing different networks were still employed, these assumptions and oversights could potentially indicate that the current model is not the most suitable model for this data. The model methods were chosen almost exclusively with subject 4 (S4) being the test set. This is reflected in the results, where predictions for S4 are more accurate and precise. Though hyperparameter tuning was performed with consideration for all three subjects, either S1 and S2 predict very well for S4, or the networks are still more fundamentally inclined to benefit that subject.

The objectives for this study were to achieve a classification system with accuracy greater than 90%, precision greater than 75%, and recall greater than 60%. These values were optimistically chosen when considering the confusion matrix of subject 4 during the initial model training with walking data (accuracy 85.5%, precision 69.9%, and recall 43.4%). With more data and finer tuning, such goals may have been achieved. However, at that stage, it was understood that the traditional approach of analyzing model performance by the sample was not practical. A stumble classification could be 0.01 s early and be considered a FP, and the stumble markings were never intended to perfectly extend to the end of each stumble. In fact, it became clear that the end of a stumble may be more difficult to ascertain and classify than the beginning. It was therefore understood that more realistic metrics would address not samples, but stumble inductions and complete gait cycles for performance. According to these new “instance” definitions, the model’s performance on each subject averaged 66.9% accuracy, 33.8% precision, and 49.6% recall. This is a decrease for the traditional model metrics and below the objectives of this study. By these standards, the hypothesis of the study was unsupported by the results. However, for practical application, this result may still be improved with the implantation of a robust control system.

4.3. Limitations

This study was intentionally restricted to common kinematic sensors, as described in the Gait Data (Section 1.1) of the introduction. Though this was done to showcase the ML model's capabilities with currently used methods, it does mean that the stumble classification is limited to detection after initiation. Future integration of peripheral sensors to measure the environment may well predict stumbles. However, the demonstrated reaction time of less than 0.1 s indicates promise in this method.

A fundamental constraint of the ML model is the dataset of the three subjects. Though more subjects were scheduled, initial COVID-19 lockdowns prevented further data collection. Artificial data and data-cleaning methods were used, but the fact remains that ML models require high-quality and labeled data, and more diverse datasets yield more beneficial models. More data were collected during subsequent trials, but these data were not available to train this model.

Because the control systems of commercial knees are proprietary, there are no direct comparisons that can be made for the evaluation of the ML model. Therefore, the limitation is that a "Simple Rule" model had to be developed to be used as a baseline comparison. However, the score achieved by this system is not meant to be seen as representative of what commercial systems would be able to achieve, but rather as standard against which the new ML models could be evaluated.

Further, many different approaches were attempted, and data were processed and reprocessed several times. It is not clear whether the current model is the absolute best model for the data as it is applied currently. Additionally, the low number of subjects potentially restricted the model selection with overfitting of the general parameter selection process. Therefore, though the model has performed admirably, it may be constrained to data similar to the training data.

4.4. Future Work

Future work would include revisiting the model selection process and hyperparameter tuning to validate the model and parameter choices with all data transformations, such as feature selection, data cleaning, artificial data, and stumble mode combination.

Exploration of the data gathered in subsequent trials would likely improve the model's performance. With the early limitation of subjects during the initial trials, the expansion of the dataset provides an opportunity to greatly improve the classification model and parameter choices. Additional methods, such as ensembling and transfer learning, warrant further investigation. Particularly for ensembling, a feature selection method should be applied. The current system uses twelve channels of data, but it is unclear whether all of these are useful, or whether some of the calculated data, such as angle or knee velocity, could not replace and improve on the current features. With proper feature selection, there is the possibility of a more accurate and more compact model. If the networks could be made smaller, the possibility of multiple parallel ensembled models in real time could result in greater network performance. Overall, this research establishes the base protocol, but there are many avenues for exploration for continued work with this dataset.

4.5. Broader Implications

Time series data classification is no new task, and several studies have suggested networks that can be implemented in real time either because of their usefulness or because their architecture was designed to be low-impact. The deployed network demonstrated in this study was not only designed to be deployed in real time but was successfully deployed in later studies. Additionally, as the HuGaDB initial classification suggested, the activities of standing, sitting, and running are accurately classifiable by the LSTM architecture. Future work should include an expansion of the classes for more versatile knee applications.

A fundamental shift in the research occurred during the model development process and display of the data. Though traditional sample-based analysis is a comfortable and known quantity, it does not necessarily apply to all datasets. For this study, it became

apparent that sample-based metrics were giving much higher accuracy than was realistic. The imbalance of classes especially contributed to this. A new perspective on the data was developed and applied in subsequent work, but continued, future analysis of this data should be conducted. Different tuning methods should be implemented, such as utilizing a cost matrix with custom weights with penalties and rewards for step metrics, and the data should be retrained according to this different set of metrics. This would allow for more customized tuning based on the perceived costs of certain types of errors.

5. Conclusions

In this study, a ML method for classifying three different forms of induced walking stumbles was demonstrated for above-knee amputees. Though the ML performance was limited by data size and quality, the study suggests the viability of implementing ML in knee prostheses to reduce stumble rates. This initial trial demonstrates the feasibility of the gathered dataset to train ML models for gait analysis. This research also provides an expanded, label-rich dataset for the analytics community, based upon which future work can be created and expanded. The modeling methods and resulting performance outlined in this study are the first iterations using this data to predict stumble events in amputee gait patterns. The accuracy of the model suggests plausible incorporation into prosthetic knees using standard IMU hardware. Additionally, the classification of stumbles happened shortly after stumble initiation, which sets the stage for feasible real-time integration to prevent stumbles from turning into falls. Further research has been conducted in this area to expand both data collection and quality, as well as modeling approaches. Follow-up work also includes integrating such methods into prosthetic devices to determine stumble control in real-time gait.

Author Contributions: Conceptualization, L.G., O.F. and R.V.G.; methodology, L.G. and R.V.G.; software, L.G. and O.F.; validation, L.G. and O.F.; formal analysis, L.G. and O.F.; investigation, L.G.; resources, L.G. and R.V.G.; data curation, L.G.; writing—original draft preparation, L.G.; writing—review and editing, L.G., O.F. and R.V.G.; visualization, L.G.; supervision, L.G. and R.V.G.; project administration, R.V.G.; funding acquisition, L.G. and R.V.G. All authors have read and agreed to the published version of the manuscript.

Funding: The research reported in this paper was supported by the National Institute of General Medical Sciences of the National Institutes of Health under linked award numbers RL5GM118969, TL4GM118971, and UL1GM118970. The content is solely the responsibility of the authors and does not necessarily represent the official views of the National Institutes of Health.

Institutional Review Board Statement: The study was conducted in accordance with the Declaration of Helsinki and approved by the Institutional Review Board of The University of Texas at El Paso (1329153-3, 30 October 2019).

Informed Consent Statement: Informed consent was obtained from all subjects involved in the study.

Data Availability Statement: The dataset presented in this study are openly available in FigShare at <https://doi.org/10.6084/m9.figshare.25308943> (accessed on 24 February 2024).

Acknowledgments: Lucas Galey thanks Edmundo Corchado CP and Sherie Ford CP from the Hanger Clinic of El Paso for their support in fitting and recruiting subjects for this study, as well as Antonio Barron for his assistance in data collection.

Conflicts of Interest: The authors declare no conflicts of interest. The funders had no role in the design of the study, in the collection, analyses, or interpretation of data, in the writing of the manuscript, or in the decision to publish the results.

References

1. Torrealba, R.R.; Fonseca-Rojas, E.D. Toward the Development of Knee Prostheses: Review of Current Active Devices. *Appl. Mech. Rev.* **2019**, *71*, 030801. [\[CrossRef\]](#)
2. Wen, Y.; Brandt, A.; Liu, M.; Huang, H.; Si, J. Comparing Parallel and Sequential Control Parameter Tuning for a Powered Knee Prosthesis Joint Department of Biomedical Engineering. In Proceedings of the 2017 IEEE International Conference on Systems, Man, and Cybernetics, Banff, AB, Canada, 5–8 October 2017; pp. 1716–1721.
3. Miller, W.C.; Deathe, A.B.; Speechley, M.; Koval, J. The Influence of Falling, Fear of Falling, and Balance Confidence on Prosthetic Mobility and Social Activity among Individuals with a Lower Extremity Amputation. *Arch. Phys. Med. Rehabil.* **2001**, *82*, 1238–1244. [\[CrossRef\]](#)
4. Hafner, B.J.; Willingham, L.L.; Buell, N.C.; Allyn, K.J.; Smith, D.G. Evaluation of Function, Performance, and Preference as Transfemoral Amputees Transition From Mechanical to Microprocessor Control of the Prosthetic Knee. *Arch. Phys. Med. Rehabil.* **2007**, *88*, 207–217. [\[CrossRef\]](#)
5. Kahle, J.T.; Highsmith, M.J.; Hubbard, S.L. Comparison of Nonmicroprocessor Knee Mechanism versus C-Leg on Prosthesis Evaluation Questionnaire, Stumbles, Falls, Walking Tests, Stair Descent, and Knee Preference. *J. Rehabil. Res. Dev.* **2008**, *45*, 1–14. [\[CrossRef\]](#)
6. Highsmith, M.J.; Kahle, J.T.; Bongiorno, D.R.; Sutton, B.S.; Groer, S.; Kaufman, K.R. Safety, Energy Efficiency, and Cost Efficacy of the C-Leg for Transfemoral Amputees: A Review of the Literature. *Prosthet. Orthot. Int.* **2010**, *34*, 362–377. [\[CrossRef\]](#)
7. Gard, S.A. Use of Quantitative Gait Analysis for the Evaluation of Prosthetic Walking Performance. *JPO J. Prosthet. Orthot.* **2006**, *18*, P93–P104. [\[CrossRef\]](#)
8. White, R.; Agouris, I.; Selbie, R.D.; Kirkpatrick, M. The Variability of Force Platform Data in Normal and Cerebral Palsy Gait. *Clin. Biomech.* **1999**, *14*, 185–192. [\[CrossRef\]](#)
9. Benedetti, M.G.; Piperno, R.; Simoncini, L.; Bonato, P.; Tonini, A.; Giannini, S. Gait Abnormalities in Minimally Impaired Multiple Sclerosis Patients. *Mult. Scler.* **1999**, *5*, 363–368. [\[CrossRef\]](#)
10. Kelleher, K.J.; Spence, W.; Solomonidis, S.; Apatsidis, D. The Characterisation of Gait Patterns of People with Multiple Sclerosis. *Disabil. Rehabil.* **2010**, *32*, 1242–1250. [\[CrossRef\]](#)
11. Wise, K.D.; Anderson, D.J.; Hetke, J.F.; Kipke, D.R.; Najafi, K. Wireless Implantable Microsystems: High-Density Electronic Interfaces to the Nervous System. *Proc. IEEE* **2004**, *92*, 76–97. [\[CrossRef\]](#)
12. Alaqtash, M.; Sarkodie-Gyan, T.; Yu, H.; Fuentes, O.; Brower, R.; Abdelgawad, A. Automatic Classification of Pathological Gait Patterns Using Ground Reaction Forces and Machine Learning Algorithms. In Proceedings of the Annual International Conference of the IEEE Engineering in Medicine and Biology Society, EMBS, Boston, MA, USA, 30 August–3 September 2011; Volume 2011, pp. 453–457.
13. Mannini, A.; Trojaniello, D.; Cereatti, A.; Sabatini, A.M. A Machine Learning Framework for Gait Classification Using Inertial Sensors: Application to Elderly, Post-Stroke and Huntington’s Disease Patients. *Sensors* **2016**, *16*, 134. [\[CrossRef\]](#)
14. Tahir, N.M.; Manap, H.H. Parkinson Disease Gait Classification Based on Machine Learning Approach. *J. Appl. Sci.* **2012**, *12*, 180–185. [\[CrossRef\]](#)
15. Badawi, A.A.; Al-Kabbany, A.; Shaban, H. Multimodal Human Activity Recognition From Wearable Inertial Sensors Using Machine Learning. In Proceedings of the 2018 IEEE-EMBS Conference on Biomedical Engineering and Sciences (IECBES); Institute of Electrical and Electronics Engineers (IEEE), Sarawak, Malaysia, 3–6 December 2018; pp. 402–407.
16. Keçeci, A.; Yildirak, A.; Özyazici, K. Gait Recognition via Machine Learning. In Proceedings of the International Conference on Cyber Security and Computer Science (ICONCS’18), Safranbolu, Turkey, 18–20 October 2018.
17. Chereshevnev, R.; Kertész-Farkas, A. *HuGaDB: Human Gait Database for Activity Recognition from Wearable Inertial Sensor Networks*; Springer International Publishing: Berlin/Heidelberg, Germany, 2018; Volume 10716.
18. Grabiner, M.D.; Koh, T.J.; Lundin, T.M.; Jahng, D.W. Kinematics of Recovery from a Stumble. *J. Gerontol.* **1993**, *48*, 97–102. [\[CrossRef\]](#)
19. Schillings, A.M.; Van Wezel, B.M.H.; Duysens, J. Mechanically Induced Stumbling during Human Treadmill Walking. *J. Neurosci. Methods* **1996**, *67*, 11–17. [\[CrossRef\]](#)
20. Cordero, A.F.; Koopman, H.J.F.M.; Van Der Helm, F.C.T. Mechanical Model of the Recovery from Stumbling. *Biol. Cybern.* **2004**, *91*, 212–220. [\[CrossRef\]](#)
21. Lawson, B.E.; Varol, H.A.; Sup, F.; Goldfarb, M. Stumble Detection and Classification for an Intelligent Transfemoral Prosthesis. In Proceedings of the 2010 Annual International Conference of the IEEE Engineering in Medicine and Biology Society, EMBC’10, Buenos Aires, Argentina, 31 August–4 September 2010; pp. 511–514. [\[CrossRef\]](#)
22. Forner-Cordero, A.; Ackermann, M.; De Lima Freitas, M. A Method to Simulate Motor Control Strategies to Recover from Perturbations: Application to a Stumble Recovery during Gait. In Proceedings of the Annual International Conference of the IEEE Engineering in Medicine and Biology Society, EMBS, Boston, MA, USA, 30 August–3 September 2011; pp. 7829–7832.
23. Hajj Chehade, N.; Ozisik, P.; Gomez, J.; Ramos, F.; Pottie, G. Detecting Stumbles with a Single Accelerometer. In Proceedings of the Annual International Conference of the IEEE Engineering in Medicine and Biology Society, EMBS, San Diego, CA, USA, 28 August–1 September 2012; pp. 6681–6686.
24. Yoo, D.; Seo, K.H.; Lee, B.C. The Effect of the Most Common Gait Perturbations on the Compensatory Limb’s Ankle, Knee, and Hip Moments during the First Stepping Response. *Gait Posture* **2019**, *71*, 98–104. [\[CrossRef\]](#)
25. King, S.T.; Eveld, M.E.; Martínez, A.; Zelik, K.E.; Goldfarb, M. A Novel System for Introducing Precisely-Controlled, Unanticipated Gait Perturbations for the Study of Stumble Recovery. *J. Neuroeng. Rehabil.* **2019**, *16*, 69. [\[CrossRef\]](#)

26. Blumentritt, S.; Schmalz, T.; Jarasch, R. The Safety of C-Leg: Biomechanical Tests. *J. Prosthet. Orthot.* **2009**, *21*, 2–15. [CrossRef]
27. Kaufman, K.; Anderson, T.; Schneider, G.; Walsh, K.; Bme, M.S. Mechanisms of Stumble Recovery: Non-Microprocessor Controlled Compared to Microprocessor-Controlled Prosthetic Knees. In Proceedings of the 34th Annual Meeting & Scientific Symposium of the American Academy of Orthotists & Prosthetists, Orlando, FL, USA, 27 February–1 March 2008.
28. Crenshaw, J.R.; Kaufman, K.R.; Grabiner, M.D. Trip Recoveries of People with Unilateral, Transfemoral or Knee Disarticulation Amputations: Initial Findings. *Gait Posture* **2013**, *38*, 534–536. [CrossRef]
29. Hak, L.; Van Dieën, J.H.; Van Der Wurff, P.; Prins, M.R.; Mert, A.; Beek, P.J.; Houdijk, H. Walking in an Unstable Environment: Strategies Used by Transtibial Amputees to Prevent Falling during Gait. *Arch. Phys. Med. Rehabil.* **2013**, *94*, 2186–2193. [CrossRef]
30. Sessoms, P.H.; Wyatt, M.; Grabiner, M.; Collins, J.D.; Kingsbury, T.; Thesing, N.; Kaufman, K. Method for Evoking a Trip-like Response Using a Treadmill-Based Perturbation during Locomotion. *J. Biomech.* **2014**, *47*, 277–280. [CrossRef]
31. Highsmith, M.J.; Kahle, J.T.; Shepard, N.T.; Kaufman, K.R. The Effect of the C-Leg Knee Prosthesis on Sensory Dependency and Falls During Sensory Organization Testing. *Technol. Innov.* **2014**, *15*, 343–347. [CrossRef]
32. Shirota, C.; Simon, A.M.; Kuiken, T.A. Transfemoral Amputee Recovery Strategies Following Trips to Their Sound and Prosthesis Sides throughout Swing Phase. *J. Neuroeng. Rehabil.* **2015**, *12*, 79. [CrossRef]
33. Bellmann, M.; Köhler, T.M.; Schmalz, T. Comparative Biomechanical Evaluation of Two Technologically Different Microprocessor-Controlled Prosthetic Knee Joints in Safety-Relevant Daily-Life Situations. *Biomed. Tech.* **2019**, *64*, 407–420. [CrossRef] [PubMed]
34. Shawen, N.; Lonini, L.; Mummidisetty, C.K.; Shparii, I.; Albert, M.V.; Kording, K.; Jayaraman, A. Fall Detection in Individuals with Lower Limb Amputations Using Mobile Phones: Machine Learning Enhances Robustness for Real-World Applications. *JMIR mHealth uHealth* **2017**, *5*, e151. [CrossRef] [PubMed]
35. Maqbool, H.F.; Husman, M.A.B.; Awad, M.I.; Abouhossein, A.; Iqbal, N.; Dehghani-Sanij, A.A. A Real-Time Gait Event Detection for Lower Limb Prosthesis Control and Evaluation. *IEEE Trans. Neural Syst. Rehabil. Eng.* **2017**, *25*, 1500–1509. [CrossRef] [PubMed]
36. Hanlon, M.; Anderson, R. Real-Time Gait Event Detection Using Wearable Sensors. *Gait Posture* **2009**, *30*, 523–527. [CrossRef] [PubMed]
37. Lambrecht, S.; Harutyunyan, A.; Tanghe, K.; Afschrift, M.; De Schutter, J.; Jonkers, I. Real-Time Gait Event Detection Based on Kinematic Data Coupled to a Biomechanical Model. *Sensors* **2017**, *17*, 671. [CrossRef] [PubMed]
38. Rueterbories, J.; Spaich, E.G.; Larsen, B.; Andersen, O.K. Methods for Gait Event Detection and Analysis in Ambulatory Systems. *Med. Eng. Phys.* **2010**, *32*, 545–552. [CrossRef] [PubMed]
39. Marayong, P.; Khoo, I.-H.; Krishnan, V.; Sciortino, A.; Crews, D.J. *Real-Time Estimation of Knee Angle, Heel-Strike, and Toe-Off Events for Gait Rehabilitation Devices*; California State University: Fullerton, CA, USA, 2017.
40. Galey, L.; Beckmann, G.; Ramos, E.; Rangel, F.A.; Gonzalez, R.V. Optimization of a Cost-Constrained, Hydraulic Knee Prosthesis Using a Kinematic Analysis Model. *Biomechanics* **2023**, *3*, 493–510. [CrossRef]
41. Sagawa, Y.; Turcot, K.; Armand, S.; Thevenon, A.; Vuillerme, N.; Watelain, E. Biomechanics and Physiological Parameters during Gait in Lower-Limb Amputees: A Systematic Review. *Gait Posture* **2011**, *33*, 511–526. [CrossRef] [PubMed]
42. Seel, T.; Raisch, J.; Schauer, T. IMU-Based Joint Angle Measurement for Gait Analysis. *Sensors* **2014**, *14*, 6891–6909. [CrossRef] [PubMed]
43. Torrealba, R.R.; Pérez-D’Arpino, C.; Cappelletto, J.; Fermín-León, L.; Fernández-López, G.; Grieco, J.C. Through the Development of a Biomechatronic Knee Prosthesis for Transfemoral Amputees: Mechanical Design and Manufacture, Human Gait Characterization, Intelligent Control Strategies and Tests. In Proceedings of the IEEE International Conference on Robotics and Automation, Anchorage, AK, USA, 3–8 May 2010; pp. 2934–2939.
44. Miyazaki, S. Long-Term Unrestrained Measurement of Stride Length and Walking Velocity Utilizing a Piezoelectric Gyroscope. *IEEE Trans. Biomed. Eng.* **1997**, *44*, 753–759. [CrossRef] [PubMed]
45. Boonstra, A.M.; Fidler, V.; Eisma, W.H. Walking Speed of Normal Subjects and Amputees: Aspects of Validity of Gait Analysis. *Prosthet. Orthot. Int.* **1993**, *17*, 78–82. [CrossRef]
46. Kumar, N.; Soni, S.; Kumar, A.; Sohi, B.S. Low Cost Prototype Development of Electronic Knee. *Ind. Res.* **2010**, *69*, 444–448.
47. Chelius, G.; Braillon, C.; Pasquier, M.; Horvais, N.; Gibollet, R.P.; Espiau, B.; Azevedo Coste, C. A Wearable Sensor Network for Gait Analysis: A Six-Day Experiment of Running through the Desert. *IEEE/ASME Trans. Mechatron.* **2011**, *16*, 878–883. [CrossRef]
48. Hochreiter, S.; Schmidhuber, J. Long short-term memory. *Neural Comput.* **1997**, *9*, 1735–1780. [CrossRef]
49. Mittal, A. Understanding RNN and LSTM. What Is Neural Network? Available online: <https://aditi-mittal.medium.com/understanding-rnn-and-lstm-f7cdf6dfc14e> (accessed on 23 April 2023).
50. Chollet, F. Others Keras 2015. Available online: https://keras.io/getting_started/faq/#how-should-i-cite-keras (accessed on 24 February 2024).
51. Abadi, M.; Agarwal, A.; Barham, P.; Brevdo, E.; Chen, Z.; Citro, C.; Corrado, G.S.; Davis, A.; Dean, J.; Devin, M.; et al. TensorFlow: Large-Scale Machine Learning on Heterogeneous Systems. *arXiv* **2015**, arXiv:1603.04467.
52. O’Malley, T.; Bursztein, E.; Long, J.; Chollet, F.; Jin, H.; Invernizzi, L.; Others KerasTuner 2019. Available online: <https://github.com/keras-team/keras-tuner> (accessed on 24 February 2024).
53. Pirker, W.; Katzenschlager, R. Gait Disorders in Adults and the Elderly: A Clinical Guide. *Wien. Klin. Wochenschr.* **2017**, *129*, 81–95. [CrossRef]

Disclaimer/Publisher’s Note: The statements, opinions and data contained in all publications are solely those of the individual author(s) and contributor(s) and not of MDPI and/or the editor(s). MDPI and/or the editor(s) disclaim responsibility for any injury to people or property resulting from any ideas, methods, instructions or products referred to in the content.